

NUMERICAL SIMULATION OF MAGNETRON INJECTION GUN FOR 1 MW 120 GHz GYROTRON

U. Singh [†], N. Kumar, N. Kumar, S. Tandon, H. Khatun

Gyrotron Laboratory, Microwave Tube Area
Central Electronics Engineering Research Institute (CEERI)
Council of Scientific and Industrial Research (CSIR)
Pilani, Rajasthan 333031, India

L. P. Purohit

Department of Physics
Gurukul Kangri Vishwavidyalaya
Haridwar 249404, India

A. K. Sinha

Gyrotron Laboratory, Microwave Tube Area
Central Electronics Engineering Research Institute (CEERI)
Council of Scientific and Industrial Research (CSIR)
Pilani, Rajasthan 333031, India

Abstract—A 40 A triode-type magnetron injection gun for a 1 MW, 120 GHz gyrotron has been designed. The preliminary design has been obtained by using some trade-off equations. Computer simulation has been performed by using the commercially available code EGUN and the in-house developed code MIGANS. The operating voltages of the modulating anode and the accelerating anode are 60 kV and 80 kV, respectively. The electron beam with a low transverse velocity spread ($\delta\beta_{\perp \max} = 3.3\%$) and velocity ratio, $\alpha = 1.38$ at beam current = 40 A is obtained. The simulated results of the MIG obtained with the EGUN code have been validated with another trajectory code TRAK. The results on the design output parameters obtained by these two codes were found to be in close agreement. The sensitivity study has been carried out by changing the different gun parameters to decide the fabrication tolerance.

Received 15 March 2010, Accepted 22 April 2010, Scheduled 9 July 2010

Corresponding author: U. Singh (uday.ceeri@gmail.com).

[†] Also with Department of Physics, Gurukul Kangri Vishwavidyalaya, Haridwar 249404, India.

1. INTRODUCTION

Microwave power at frequencies above about 100 GHz is used for the heating of the magnetically confined plasma in the experimental fusion devices [1, 2]. Gyrotron is an efficient device for the generation of the millimeter waves at such frequencies at the required power levels (≥ 1 MW) [3]. The gyrotron is based on the cyclotron maser interaction between the electromagnetic wave and the gyrating electron beam [4]. In the gyrotron, the source of the electron beam is a magnetron injection gun (MIG), which produces annular electron beam with the required beam parameters (Fig. 1). The cathode used in the MIG is operated under the temperature limited region to minimize the electron beam velocity spread. The electrons emitted from the cathode move in the helical path under the influence of the cross electric and magnetic fields. The efficient operation of the gyrotron depends on the quality of the electron beam. Therefore, as per requirement of the electron beam properties at the interaction region, some trade-off equations are used for the initial design of the MIG. These equations are based on the conservation of the angular momentum and the assumption of the adiabatic approximation [5–7]. By using these equations, the gun parameters such as the cathode radius (r_c), the cathode-modulating anode spacing (d_{ac}), the emitter current density (J_c), the electric field at cathode (E_c), etc. are estimated. Then the trajectory analysis codes are used for the final optimization of the electrodes and the beam properties on the basis of the operating parameters.

In India, an activity related to the design and development of 120 GHz, 1 MW gyrotron has been started. For the better performance of the gyrotron and the other gyro-devices, an electron beam of good quality is required [5–10]. A 3.2 MW triode-type electron gun has been designed for this tube. The triode-type MIG has been chosen because of its additional control on the electron beam properties. The MIG at frequency of 120 GHz has already been designed as presented elsewhere [11]. To characterize the quality of electron beam, maximum transverse

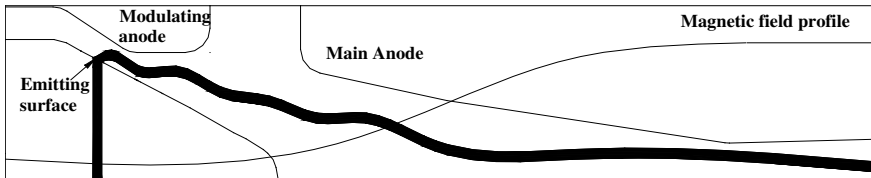


Figure 1. Schematic view of the magnetron injection gun (MIG) with electron beam profile.

velocity spread of the electron beam ($\delta\beta_{\perp\max}$) is used. The present design predicts a better beam quality with respect to $\delta\beta_{\perp\max}$ (3.3%) at $\alpha = 1.38$. To obtain the initial parameters for this MIG design, a computer program MIGSYN in C++ has been developed [12–14]. Using MIGSYN, a range of cathode radius is found and any value of the cathode radius within the range can be adopted for this MIG design. Optimization of the MIG geometry has been performed by using the commercially available code EGUN [15] and the in-house developed code MIGANS [16,17]. MIGANS is basically a post processor of the EGUN code and is used to find out the different electron beam parameters like $\alpha (= \beta_{\perp}/\beta_z)$, the maximum transverse velocity spread ($\delta\beta_{\perp\max}$), the larmor radius (r_l), etc. Here, β_{\perp} and β_z are the average transverse and axial electron velocities, respectively in the interaction region normalized to the velocity of light (c). The study has been completed with the validation of the design by using another trajectory code TRAK [18].

2. PRELIMINARY DESIGN

From the available literature on MIG [5–22], the design criteria have been set up with respect to the different parameters related to the cathode, the electron beam and the anode (Table 1). Here in Table 1, J_L is the space charge limited current density and r_{lc} is the larmor radius at cathode.

Table 1. Limits of various parameters in the MIG design.

Electric field at cathode (E_c)	$20 \text{ kV/cm} < E_c < 60 \text{ kV/cm}$
Magnetic compression ratio (f_m)	$10 < f_m < 30$
Gap factor ($D_f = d_{ac}/r_{lc}$)	> 3
Current ratio (J_c/J_l)	< 0.2
Maximum transverse velocity spread ($\delta\beta_{\perp\max}$)	$< 5\%$
Cathode angle (ϕ_c)	$> 25^\circ$
Cathode current density (J_c)	$1 \text{ A/cm}^2 < J_c < 5 \text{ A/cm}^2$
Transverse-to-axial beam velocity ratio (α)	≤ 1.5
Relativistic factor (γ_0)	$1.1 < \gamma_0 < 1.2$
Electric field breakdown (E_b) (in vacuum)	$< 5 \text{ kV/mm}$

It is envisaged to employ the gun in a 120 GHz gyrotron under development to provide 1 MW CW RF output power. The electron beam power has been estimated from the RF output power of 1 MW

by assuming an RF output efficiency of about 30%. For a selected operating mode, the interaction structure calculations determine the magnetic field at the interaction region (B_0), the accelerating beam voltage (V_0), the beam current (I_0), the average beam radius (r_b) and other beam properties at the interaction region. The mode selection depends on several parameters, namely, the voltage depression, the limiting current, the ohmic wall loading, etc., described in detail elsewhere [5, 6]. On the basis of the mode selection parameters and the start up scenario in the interaction region [23, 24], the high order TE_{22,6} mode has been selected as the operating mode and the electron beam has been launched at the first radial maxima for the fundamental beam-mode operation. The TE_{22,6} mode exhibits high coupling with the gyrating electron beam. The beam current and the beam voltage have been chosen on the basis of the interaction efficiency, the space charge effect at the interaction cavity and the velocity ratio of the electron beam [25, 26]. The nominal beam parameters at the interaction region are shown in Table 2. Further, using the design criteria presented in Table 1, the value of the magnetic compression ratio has been selected 20. The selected value of f_m is the mean of the values shown in the Table 1. Reflection of electrons at the magnetic mirror occurs when the maximum transverse velocity of the electron beam ($\beta_{\perp \max}$) approaches the total velocity (β_0). The low value of α (≤ 1.5) has been chosen [5, 6, 27] to minimize the reflection of the electrons so that, the maximum transverse velocity spread ($\delta\beta_{\perp \max}$) remain below 5%. The maximum transverse velocity spread is given by [5, 19]:

$$\delta\beta_{\perp \max} = \frac{(\beta_{\perp \max} - \beta_{\perp})}{\beta_{\perp}} \quad (1)$$

where $\beta_{\perp \max}$ and β_{\perp} are the maximum and the average values of the transverse velocity of the electron beam, respectively. The cathode-modulating anode and the modulating anode-accelerating anode spacing have been kept as such that the voltage breakdown could not occur.

Then, by using the trade-off equations derived by Baird and Lawson [12, 13], a computer program MIGSYN in C++ has been developed. A detail study has been carried out by using MIGSYN to see the effect of the cathode radius variation on the various MIG parameters. Fig. 2 shows the selection method of the cathode radius range through the observation of its variation on the gap factor (D_f), the electric field at the cathode (E_c), the magnetic compression ratio (f_m) and the current ratio (J_c/J_l). Within the tolerable limits of these parameters under the design criteria shown in Table 1, the range of the cathode radius has been selected from 46 mm to 53 mm (Fig. 2). Any value of the cathode radius within this range can be adopted for this

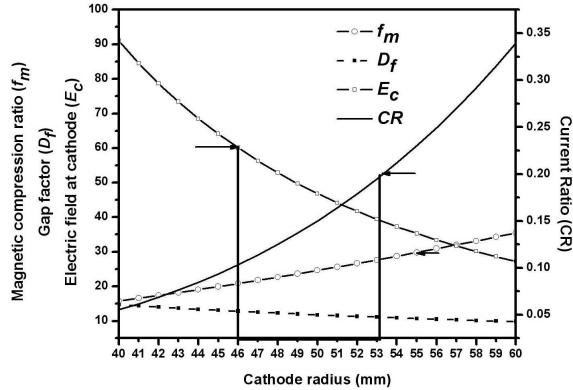


Figure 2. A typical plot showing the suitable range for setting the cathode radius satisfying all the physical constraints for the gun design.

Table 2. Nominal electron beam parameters.

Beam voltage (V_0)	80 kV
Beam current (I_0)	40 A
Output power (P_0)	1 MW
Operating mode	TE _{22,6}
Magnetic field at the interaction region (B_0)	4.82 T
Average beam radius (r_b)	10.08 mm
Transverse-to-axial beam velocity ratio (α)	≤ 1.5
Maximum transverse velocity spread ($\delta\beta_{\perp \max}$)	$< 5\%$

MIG design. Here, the design criteria regarding to the electron beam velocity spread given in Table 1 has not been used in the preliminary design, though it has been used in the electron beam analysis. Fig. 3 shows the two dimensional MIG geometry used for electron beam analysis.

For the actual synchronization of the electron beam with the RF at the interaction region, the magnetic field is always kept less than the peak magnetic field. Here, the magnetic field at the interaction region has been reduced from the peak value (4.95 T) by a factor of 2.5% giving the value of $B_0 \approx 4.82$ T. The peak value of B_0 at the interaction region has been calculated by using $B_0 = f$ (GHz) $\gamma_0/28$ s, where f is the operating frequency, γ_0 is the relativistic factor and s is the harmonic number [5, 6, 14].

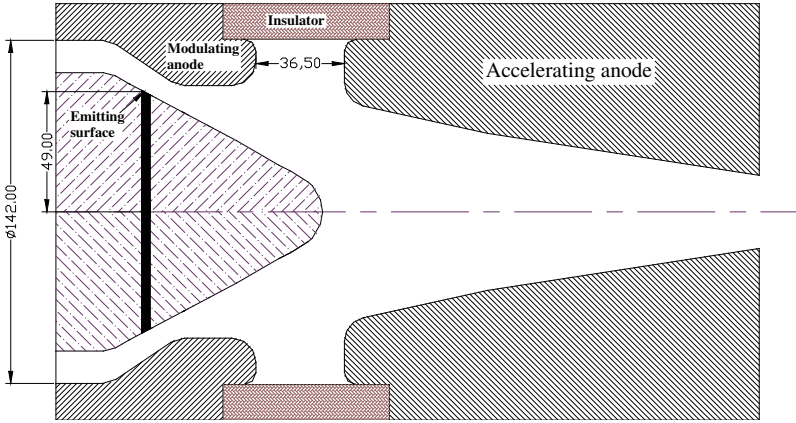


Figure 3. The two dimensional MIG geometry used for electron beam analysis.

3. SIMULATION AND DISCUSSION

Based on the preliminary design, the trajectory analysis has been carried out to optimize the electrode shapes and the electron beam parameters. Various dimensions and the parameters for the trajectory simulation are shown in Table 3. The computer simulation has been performed by using the commercially available code EGUN. The calculations have been performed with 16 beamlets. The main goal of the triode-type MIG design is to launch the electron beam at the first radial maxima of the operating mode at the interaction region with the minimum transverse velocity spread ($\delta\beta_{\perp\max}$). Considering the technical limits, first the shape of the electrodes including the emitter has been optimized for the low transverse velocity spread at the nominal beam parameters and then the electron beam parameters at the interaction region have been optimized. After numerical simulation of the MIG, the electrical parameters have been evaluated with the help of MIGANS code. The EGUN simulation has thus provided the optimized design parameters and the beam profile (Fig. 4, Table 4).

For a high current electron beam, the influence of the space charge effect on the velocity spread is an important factor. To reduce the space charge influence, ϕ (angle between the emitter surface and the magnetic field line) should be greater than 25° . In this case the laminar beam is formed and, therefore, the velocity spread growth with beam current is reduced [8–10]. Fig. 5 shows the laminar beam profile near the cathode. The calculated value of the maximum transverse velocity spread due to the electron optics is approximately 3.3% at $\alpha = 1.38$.

Table 3. Dimensions and parameters used in the trajectory simulation.

Mean radius of the emitter (r_c)	49 mm
Slant length of the emitting surface (l_s)	3.84 mm
Slope angle of the emitter (ϕ_c)	28°
Magnetic field at the interaction region (B_0)	4.82 T
Compression ratio (f_m)	20

Table 4. Optimized values of different MIG parameters.

Modulating anode voltage (V_a)	60 kV
Cathode current density	3.2 A/cm ²
Maximum transverse velocity spread ($\delta\beta_{\perp}$)	3.3%
Transverse-to-axial beam velocity ratio (α)	1.38
Average beam radius (r_b)	9.95 mm

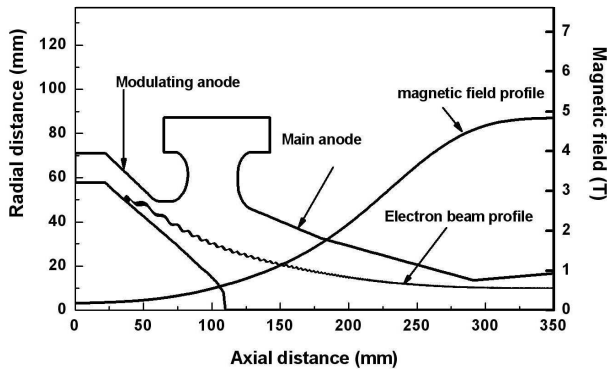


Figure 4. MIG with the electrode geometry, the beam profile and the magnetic field profile optimized by using EGUN code.

For the sake of simplicity, the influence of the surface roughness and the cathode temperature on the beam parameters has not been considered in the calculation of the maximum transverse velocity spread. This aspect will be considered in due course of time.

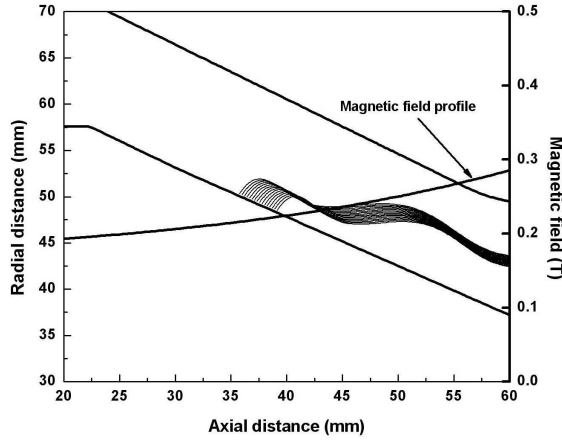


Figure 5. Optimized beam profile near the cathode by using the EGUN code.

Table 5. Comparison of the EGUN and the TRAK results.

Parameters	EGUN results	TRAK results
Transverse velocity (β_{\perp})	0.35	0.36
Transverse-to-axial beam velocity ratio (α)	1.38	1.4
Average beam radius (r_b)	9.95 mm	10 mm
Maximum transverse velocity spread ($\delta\beta_{\perp \max}$)	3.3%	3.5%

4. DESIGN VALIDATIONS

To validate the design of the MIG for 120 GHz gyrotron, another trajectory code TRAK has been used. The initial parameters and the geometry were same as used in the EGUN simulation. In the TRAK simulation, the numerical calculations have been performed with 16 beamlets. Table 5 shows the comparison of the results. The final values obtained in the TRAK simulation show good agreement with the EGUN results. Fig. 6 shows the beam profile achieved by using the TRAK code.

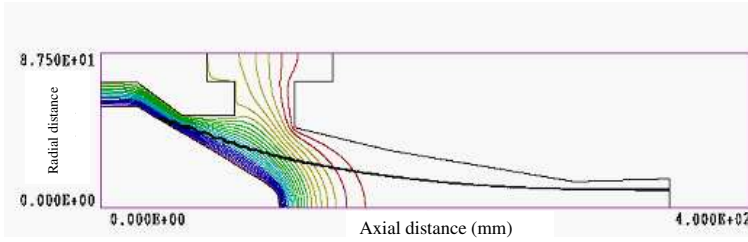


Figure 6. MIG with the electrode geometry and the beam profile optimized by using TRAK code.

5. SENSITIVITY ANALYSIS OF THE MIG PARAMETERS

During the fabrication and operation of the device, it is very difficult to maintain the MIG operating parameters fixed. A small change in the MIG parameters affects the beam-wave interaction which leads to the change in the output power. Thus, it is necessary to analyze the effect of the variation of the various gun input parameters, namely, the beam voltage (V_0), the cathode magnetic field (B_{zc}), the cavity magnetic field (B_0) and the modulating anode voltage (V_a) on the beam quality parameters (α and $\delta\beta_{\perp \max}$) (Figs. 7–10). The transverse velocity (β_{\perp}) and the transverse-to-axial beam velocity ratio (α) at the interaction region under the adiabatic condition are given by [5]:

$$\beta_{\perp} \approx \frac{1}{\gamma_0 c} f_m^{1/2} \frac{E_c \cos \phi_{eB}}{B_{zc}} = \frac{1}{\gamma_0 c} \frac{f_m^{1/2}}{B_{zc}} \frac{V_a \cos^2 \phi_{eB}}{r_c \ln(1 + D_f \mu)} \quad (2)$$

$$\alpha = \frac{\beta_{\perp}}{(1 - \gamma_0^{-2} - \beta_{\perp}^2)^{1/2}} \quad (3)$$

Here E_c is the electric field at the cathode, γ_0 is the relativistic factor, D_f is the gap factor between the cathode and the modulating anode, ϕ_{eB} is the angle between the emitter surface and the magnetic field line, r_c is the cathode radius, f_m is the magnetic compression ratio and μ is the cylindrical parameter.

The amounts of the sensitivity of α to the various gun input parameters obtained by the EGUN simulation and analytical calculations (Figs. 7(a)–10(a)) agree to a large extent. Further, the value of α and $\delta\beta_{\perp \max}$ decreases with the increase of the cavity magnetic field (Fig. 7). In adiabatic flow of the electron beam, the transverse velocity of the electron beam depends inversely on the cathode magnetic field. For a fixed magnetic compression ratio, the

value of the transverse velocity (see 2) and, consequently, the value of α decreases with the increase in the cathode magnetic field. The value of α is found to be very sensitive to the value of the cathode magnetic field, changing from 1.44 to 1.18 as the magnetic field is varied from 0.24 T to 0.25 T (Fig. 8(a)). The value of $\delta\beta_{\perp\max}$ also decreases with increase in cathode magnetic field (Fig. 8(b)). According to the scaling laws of adiabatic flow for triode-type gun, the influence of the beam voltage on the transverse component of the beam velocity is negligible [5]. But with the increase in the beam voltage, the value of the axial velocity of the electron beam increases and, consequently, the

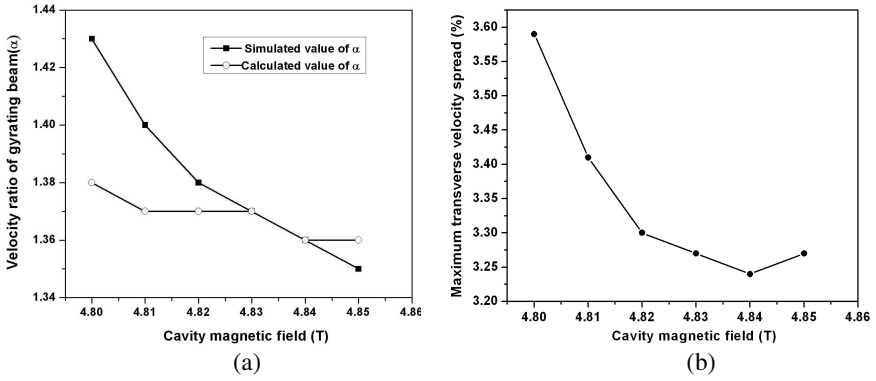


Figure 7. Effect of the cavity magnetic field variation on the beam quality parameters.

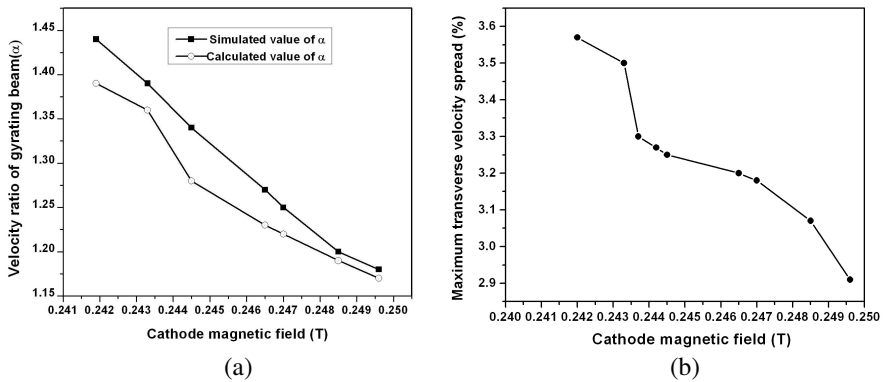


Figure 8. Effect of the cathode magnetic field variation on the beam quality parameters.

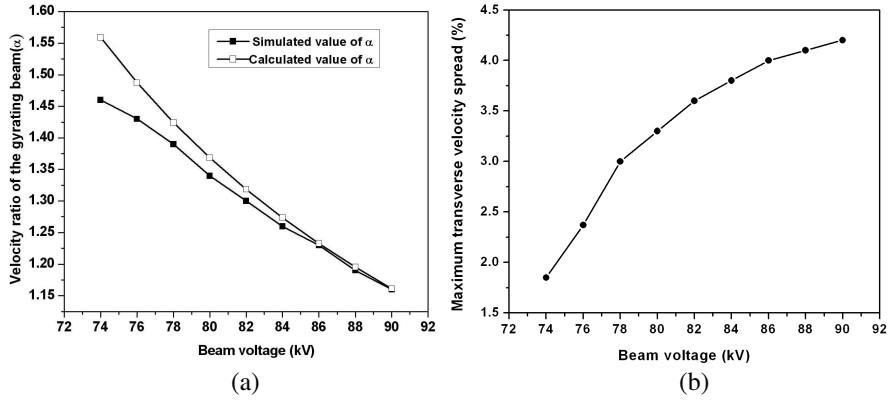


Figure 9. Effect of the beam voltage variation on the beam quality parameters.

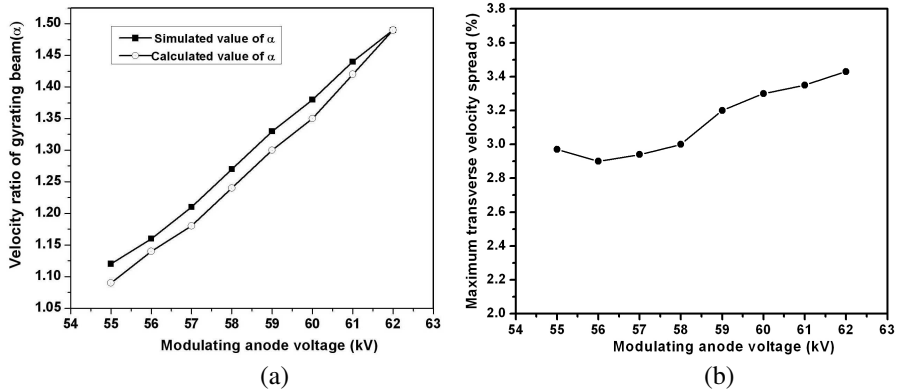


Figure 10. Effect of the modulating anode voltage variation on the beam quality parameters.

value of α decreases (Fig. 9(a)), while the value of $\delta\beta_{\perp\max}$ increases (Fig. 9(b)). Further, with the increase in the modulating anode voltage, the value of α increases appreciably (Fig. 10(a)) and, therefore, the value of $\delta\beta_{\perp\max}$ increases (Fig. 10(b)).

6. CONCLUSION

In this paper, the design of a triode-type MIG for 120 GHz, 1 MW gyrotron has been presented. The design of the MIG has been

achieved by using the adiabatic trade-off equations and the electron trajectory code EGUN. Good enough quality electron beam with a low transverse velocity spread ($\delta\beta_{\perp\max} = 3.3\%$) and $\alpha = 1.38$ at the beam voltage = 80 kV and the beam current = 40 A has been predicted. The design obtained by using the EGUN code has been validated with another electron trajectory code TRAK. Results obtained using both the codes are in good agreement. The sensitivity analysis of the MIG parameters with respect to the beam quality parameters like α and the maximum transverse velocity spread has also been analyzed. The MIG parameters like magnetic field at the cathode centre and the modulating anode voltage affect the beam quality parameters critically while the latter are less sensitive to the magnetic field at the cavity center and the beam voltage. The present sensitivity analysis is thus useful in the design of an MIG while deciding the tolerance in the electron beam and magnetic field parameters.

ACKNOWLEDGMENT

Authors are grateful to the Director, CEERI, Pilani, for permission to publish this paper. Thanks are due to Dr. S. N. Joshi, Dr. V. Srivastava, Dr. R. S. Raju and the team members for their continuous support and encouragement. Thanks are also due to Council of Scientific and Industrial Research (CSIR) for funding this project.

REFERENCES

1. Thumm, M., "High power gyro-devices for plasma heating and other applications," *Int. J. Infrared Millim. Waves*, Vol. 26, 483–503, Apr. 2005.
2. Dammertz, G., et al., "Development of multimegawatt gyrotrons for fusion plasma heating and current drive," *IEEE Trans. Plasma Sci.*, Vol. 52, No. 25, 808–817, May 2005.
3. Thumm, M., "State-of-the-art of high power gyro-devices and free electron masers update 2006," Scientific Report FZKA 7289, Forschungszentrum Karlsruhe, Karlsruhe, Germany, Feb. 2007.
4. Flyagin, V. A., A. V. Gaponov, I. Petelin, and V. K. Yulpatov, "The gyrotron," *IEEE Trans. Microwave Theory Tech.*, Vol. 25, No. 6, 514–521 1977.
5. Edgcombe, C. J., Ed., *Gyrotron Oscillators: Their Principles and Practice*, Taylor & Francis, London, 1993.
6. Kartikeyan, M. V., E. Borie, and M. Thumm, *Gyrotrons High-*

- Power Microwave and Millimeter Wave Technology*, Springer, Germany, 2004.
7. Nusinovich, G. S., *Introduction to the Physics of Gyrotrons*, Johns Hopkins University Press, Maryland, USA, 2004.
 8. Goldenberg, A. L. and M. I. Petelin, "The formation of helical electron beams in an adiabatic gun," *Izv. VUZov. Radiofizika*, Vol. 16, 141–149, 1973.
 9. Krivosheev, P. V., V. K. Lygin, V. N. Manuilov, and S. E. Tsimring, "Numerical simulation models of forming systems of intense gyrotron helical electron beams," *Int. J. of Infrared and millimeter Waves*, Vol. 22, 1119–1146, 2001.
 10. Tsimring, S. E., "Gyrotron electron beams: Velocity and energy spread and beam instabilities," *Int. J. of Infrared and millimeter Waves*, Vol. 22, 1433–1468, 2001.
 11. Choi, E. M., C. Marchewka, I. Mastovsky, M. A. Shapiro, J. R. Sirigiri, and R. J. Temkin, "Megawatt power level 120 GHz gyrotrons for ITER start-up", *Journal of Physics: Conference Series*, Vol. 25, 1–7, 2005.
 12. Baird, J. M. and W. Lawson, "Magnetron injection gun (MIG) design for gyrotron applications," *Int. J. Electronics*, Vol. 61, 953–967, 1986.
 13. Lawson, W., "MIG scaling," *IEEE Trans. Plasma Science*, Vol. 16, No. 2, 290–295, 1988.
 14. Udaybir, S., A. Bera, R. R. Rao, and A. K. Sinha, "Synthesized parameters of MIG for 200 kW, 42 GHz gyrotron," *J. of Infrared, Millimeter, and Terahertz Waves*, 1886–6906, Dec. 2009 [online].
 15. Hermannsfeldt, W. B., EGUN, Stanford Linear Accelerator Center, Stanford University Report SLAC-226, 1979.
 16. Bera, A., S. Udaybir, R. R. Rao, and A. K. Sinha, "Design of MIG for 42 GHz, 200 kW Gyrotron," *IEEE IVEC-2008*, Monterey, USA, 2008.
 17. Udaybir, S., A. Bera, N. Kumar, and A. K. Sinha, "Numerical simulation of MIG for 200 kW, 42 GHz gyrotron," *Int. J. of Infrared and millimeter Waves*, Jan. 2010 [online].
 18. TRAK 6.0, Finite-element Charged-particle Optics, Albuquerque, New Mexico 87192, U.S.A.
 19. Lygin, V. K., B. Piosczyk, G. Dammertz, A. N. Kuftin, and V. E. Zapevalov, "A diode electron gun for a 1 MW 140 GHz gyrotron," *Int. J. Electronics*, Vol. 82, No. 2, 193–201, 1997.
 20. Fliflet, A. W., A. J. Dudas, M. E. Read, and J. M. Baird, "Use of electrode synthesis technique to design MIG-type guns for high

- power gyrotrons,” *International Journal of Electronics*, Vol. 53, No. 6, 743–754, 1982.
21. Barroso, J. J., A. Montes, and C. A. B. Silva, “The use of a synthesis method in the design of gyrotron electron guns,” *International Journal of Electronics*, Vol. 59, No. 1, 33–47, 1985.
 22. Dryden, V. W., “Exact solutions for space-charge flow in spherical coordinates with application to magnetron injection guns,” *Journal of Applied Physics*, Vol. 33, 3118–3124, 1962.
 23. Danly, B. G. and R. J. Temkin, “Generalized nonlinear harmonic gyrotron theory,” *Phys. Fluids*, Vol. 29, 561–567, 1986.
 24. Borie, E. and B. Jödicke, “Comments on the linear theory of the gyrotron,” *IEEE Trans. Plasma Sci.*, Vol. 16, 116–121, 1988.
 25. Drobot, A. T. and K. Kim, “Space charge effects on the equilibrium of guided electron flow with gyromotion,” *Int. J. Electronics*, Vol. 51, 351, 1981.
 26. Ganguli, A. K. and K. R. Chu, “Limiting current in gyrotrons,” *Int. J. of Infrared and Millimeter Waves*, Vol. 5, 103, 1984.
 27. Piosczyk, B., “A novel 4.5-MW electron gun for a coaxial cavity gyrotron,” *IEEE Transactions on Electron Devices*, Vol. 48, No. 12, 2001.